PNAS

Supporting Information for

Phloretin enhances remyelination by stimulating oligodendrocyte precursor cell differentiation

Tess Dierckx[1], Sam Vanherle[1], Mansour Haidar[1], Elien Grajchen[1], Fleur Mingneau[1], Pascal Gervois[2], Esther Wolfs[2], Dany Bylemans[3,4], Arnout Voet[5], Tien Nguyen[5], Ibrahim Hamad[1,6], Markus Kleinewietfeld[1,6], Jeroen F.J. Bogie[1], Jerome J.A. Hendriks[1]*

[1]Department of Immunology and Infection, Biomedical Research Institute, Hasselt University, Diepenbeek 3590, Belgium.

[2]Group of Cardio & Organ Systems (COS), Biomedical Research Institute, Hasselt University, Diepenbeek 3590, Belgium.

[3]Research Station for Fruit Cultivation, Sint-Truiden 3800, Belgium.

[4]Department of Biosystems, KU Leuven, Heverlee 3001, Belgium.

[5]Department of Chemistry, Laboratory for Biomolecular Modelling and Design, KU Leuven, Heverlee 3001, Belgium.

[6]VIB Laboratory of Translational Immunomodulation, VIB Center for Inflammation Research, Hasselt University, Diepenbeek 3590, Belgium.

*To whom correspondence should be addressed: Jerome J.A. Hendriks, Jerome.hendriks@uhasselt.be

This PDF file includes:

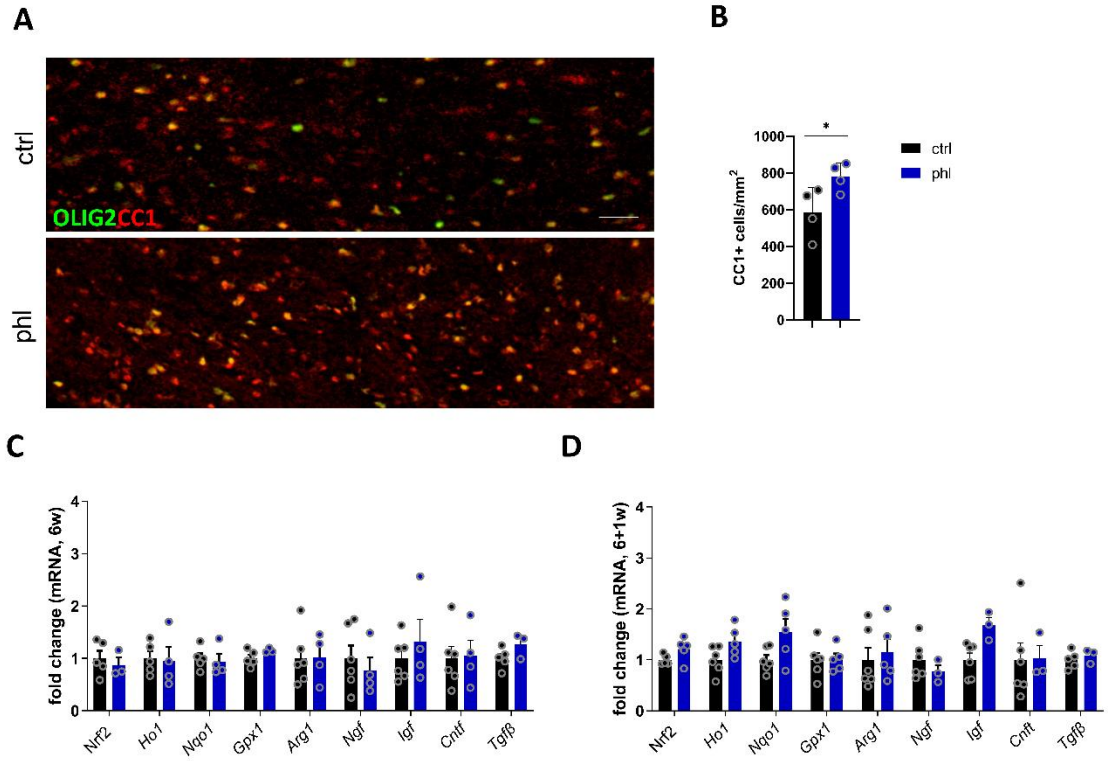

Supplementary Fig. 1 Oligodendrocytes numbers and inflammatory mediator expression in the corpus callosum of phloretin-treated cuprizone animals. A-B. Representative images and quantification of the OLIG2/CC1 staining in the corpus callosum (CC) from control- or phloretin-treated mice (n=4) after cuprizone withdrawal (6+1w). Scale bar, 50 µm **C-D.** mRNA expression of anti-inflammatory mediators in the CC of vehicle- or phloretin-treated mice at 6w and 6+1w. Ctrl, control; phl, phloretin. Data are represented as mean ± s.e.m.

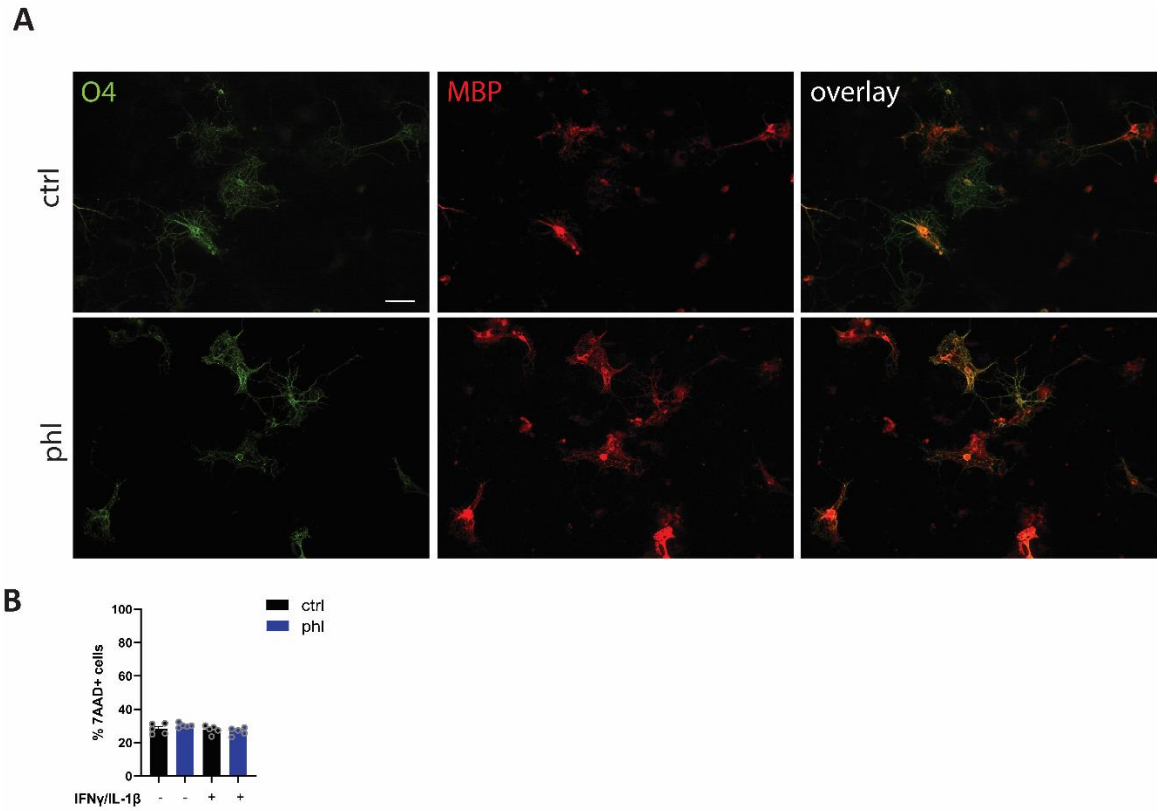

Supplementary Fig. 2 Phloretin induces oligodendrocyte precursor cell maturation. A. Representative images of vehicle- and phloretin-treated oligodendrocyte precursor cell (OPC) cultures in low magnification. Scale bar, 25 µm. **B.** Viability of vehicle- and phloretin-treated OPCs stimulated with or without IFNγ/IL-1β (n=5). Ctrl, control; phl, phloretin.

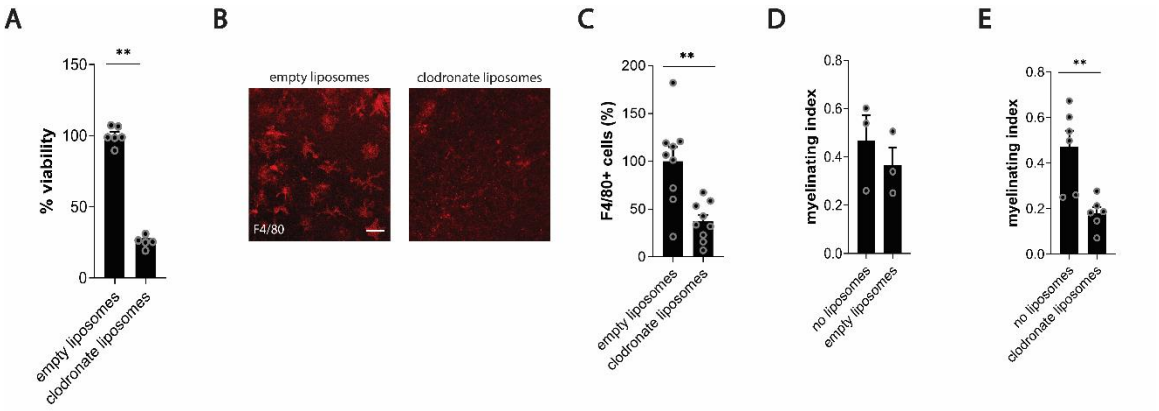

Supplementary Fig. 3 Clodronate liposomes deplete phagocytes in vitro and ex vivo. A. Viability levels of bone marrow derived macrophages treated with clodronate liposomes or empty liposomes, demonstrating the macrophage-depletion ability of clodronate liposomes (n=5-6). **B-C.** Representative images and quantification of F4/80+ cells in ex vivo cerebellar brain slice cultures (BSCs), illustrating clodronate liposomes-mediated microglia depletion (n=9). Scale bar, 25 µm **D.** Remyelination index of empty liposomes-treated BSCs compared to control BSCs (n=3) **E.** Remyelination index of microglia-depleted BSCs compared to control BSCs (n=6). Ctrl, control; phl, phloretin. Data are represented as mean ± s.e.m. **p < 0.01 (unpaired t-test, two-tailed).

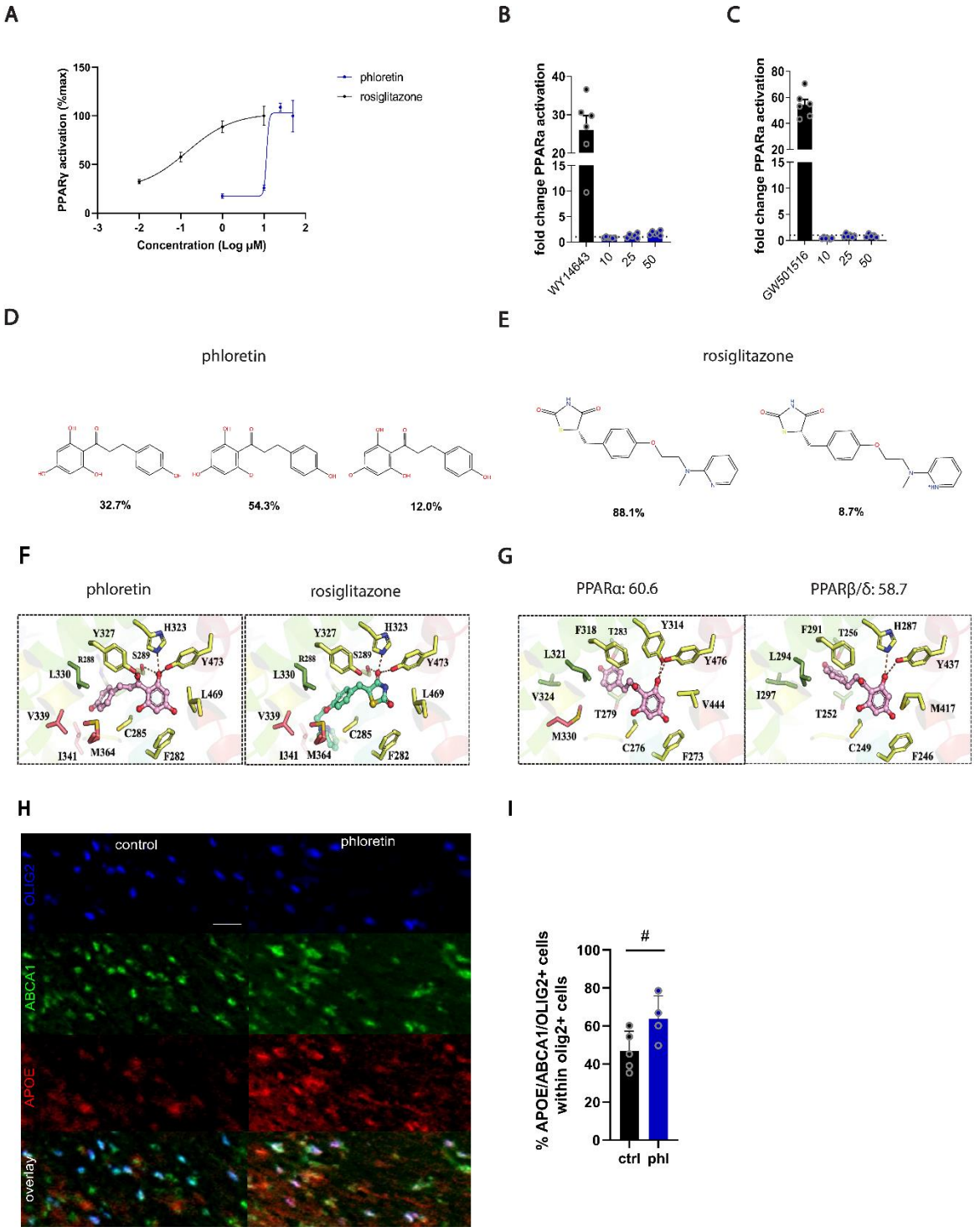

Supplementary Fig. 4 Phloretin is a potent peroxisome proliferator-activated receptor γ ligand. A. EC50 values of phloretin (11.61 μM) and rosiglitazone (0.1427 μM) for PPARγ activation. **B-C.** Results of the potent peroxisome proliferator-activated receptor α (PPARα) and PPARβ/δ ligand-binding luciferase assay in cos7 cells stimulated with different phloretin concentrations or the PPAR-isoform specific agonist (n=6) **D-E.** 3D protonation states of phloretin and rosiglitazone at pH 7. The dominant state of phloretin and rosiglitazone accounts for 54.3 % and 88.1 %, respectively. The dominant state was used in the 3D conformations. **F.** Molecular docking poses of phloretin and rosiglitazone in PPARγ binding domain. The PPAR ligand binding domain (LBD) consists of three arms (I,II,III) which are shown in yellow, pink, and green

sticks respectively. The overall binding mode of phloretin is similar to that of rosiglitazone, with the exception of the elongated pyridine group of rosiglitazone. The head group of phloretin and rosiglitazone forms a hydrogen bond network with the LBD residues Ser289, His323, and Tyr473, and their central benzene rings interact with the hydrophobic residues Cys285, Leu330, and Met364. **G.** Phloretin makes a hydrogen bonding network with arm I's residues Tyr314 and Tyr476, and hydrophobic interactions with arm III's residues Thr279, Thr283, Leu321 and Val324, and arm II's residue Met330 in the PPARα LBD. In the PPARβ/δ LBD, phloretin makes a hydrogen bonding network with arm I's residues His287 and Tyr437, and hydrophobic interactions with arm III's residues Thr252, Thr256, Leu294 and Ile297. Binding affinity of phloretin in the LBD of PPARα and PPARβ/δ are 60.6011 and 58.6536 respectively. **H-I.** Representative images and quantification of the OLIG2/ABCA1/APOE staining in the corpus callosum (CC) from control- or phloretin-treated mice (n=4) after cuprizone withdrawal (6+1w). Scale bar, 50 µm. Ctrl, control; phl, phloretin. Data are represented as mean ± s.e.m. #p=0.05 (unpaired t-test, two-tailed).

Supplementary Table 1. List of primer sequences used for qPCR.

Gene	Forward	Reverse
Ccl5	GGAGTATTTCTACACCAGCACGCAA	GCGGTTCCTTCGAGTGACA
Nos2	AAAAACCCTTGTGCTGTTCTC	ATACTGTGGACGGGTCGATG
Ccl4	GAAGCTTTGTGATGGATTACTATGAGA	GTCTGCCTCTTTTGGTCAGGA
Il6	TGTCTATACCACTTCACAAGTCGGAG	GCACAACTCTTTTCTCATTTCCAC
Il1β	ACCCTGCAGCTGGAGAGTGT	TTGACTTCTATCTTGTTGAAGACAAACC
Tnfα	CCAGACCCTCACACTCAG	CACTTGGTGGTTTGCTACGAC
Mbp	TCACAGAAGAGACCCTCACAGC	GAGTCAAGCATGCCCGTGTC
Plp	TTGTTTGGGAAAATGGCTAGG	GCAGATCGACAGAAGCTTGGA
Abca1	CCCAGAGCAAAAAGCGACTC	GGTCATCATCACTTTGGTCCTTG
Cpta1	GGAGGTTGTCCACGAGCCAG	TCATCAGCAACCGGCCCAAA
Apoe	CCTGAACCGCTTCTGGGATT	GCTCTTCCTGGACCTGGTCA
Cd36	GGACATTGAGATTCTTTTCCTCTG	GCAAAGGCATTGGCTGGAAGAAC
Nrf2	CGAGATATACGCAGGAGAGGTAAGA	GCTCGACAATGTTCTCCAGCTT
Ho1	GCCGAGAATGCTGAGTTCATG	TGGTACAAGGAAGCCATCACC
Nqo1	CGCCTGAGCCCAGATATTGT	GCACTCTCTCAAACCAGCCT
Gpx1	GACACCAGGAGAATGGCAAGA	TCACCATTCACTTGGCACTTC
Arg1	GTGAAGAACCCACGGTCTGT	GCCAGAGATGCTTCCAACTG
Ngf	GGAGCGCATCGAGTTTTGG	TCCTTGGCAAAACCTTTATTGGG
Igf	TACTTCAACAAGCCCACAGGC	ATAGAGCGGGCTGCTTTTGT
Cntf	TCTGTAGCCGCTCTATCTGG	GGTACACCATCCACTGAGTCAA
Tgfβ	GGGCTACCATGCCAACTTCTG	GAGGGCAAGGACCTTGCTGTA